Expert Design Evaluation System for Injection Molding

Sang-Gook Kim[1], Yong-Jeong Huh[2]

[1] School of mechanical engineering, Massachusetts Institute of Technology, USA
[2] School of mechatronics engineering, Korea University of Technology and Education ChungNam, South Korea

ABSTRACT

The design and manufacture of injection molded polymeric parts with desired properties is a costly process dominated by empiricism, including the repeated modification of actual tooling. This paper presents an expert design evaluation system which can predict the mechanical performance of a molded product and diagnose the design before the actual mold is machined. The knowledge-based system synergistically combines a rule-based expert system with CAE programs. An iterative boundary pressure reflection method (IBPR) is developed to automate the cavity filling simulation program and to predict thermo-mechanical properties of a molded part precisely. Mathematical models of weldline and frozen-in molecular orientation are established to determine the spatial variation of microstructural anisotropies of a molded part from the result of cavity filling simulation. The strength ellipse is devised as an index which represents the spatial distribution of the microstructural anisotropies of a molded part. Heuristic knowledge of injection molding, flow simulation, and mechanical performance prediction is formalized as rules of an expert consultation system. The expert system interprets the analytical results of the process simulation, predicts the performance, evaluates the design and generates recommendations for optimal design alternatives.

Keywords : Expert design evaluation system, injection molding, flow simulation, mechanical performance, knowledge formalization

1. Rational Design in Injection Molding

Design is, within the scope of engineering applications, a hierarchical series of transformation processes from a functional description of a product to a physical entity [1,2].

The design task is to specify the physical components, the geometry and the processes required to manufacture a product which performs a desired set of functions needed by a user. The design process involves creative, analytical, theoretical and experimental work in a complex, iterative and recursive manner. In this respect, the object of rational design is to make the specifications such that the designing, production and utilization of the product consume a minimum of resources and information [3]. A rational design strategy differs from an exhaustive generation-and-test problem-solving technique [4], in that it has criteria for evaluating design decisions and indices for generating design alternatives prior to the expensive and time-consuming prototype toolings.

Some of the major manufacturing processes often deteriorate the quality of the product significantly unless the manufacturability is not considered adequately in the part design. Injection molding, for example, generates a complicated distribution of the microstructure as determined by the choice of processing conditions, material, and configuration of the part and mold. Therefore, it requires the designer to have in-depth knowledge about the nature of the injection molding process to produce a successful injection molded product. An incomplete understanding of the process could result in product designs which have unacceptable properties or which cannot even be moldable.

Injection molding is a process by which plastic pellets or powders are melted and pressurized into a cavity to form a complex three dimensional part in a

single cyclic operation. The engineering tasks involved in injection molding are the creation of the geometry of parts and molds, and the choice of material and processing parameters. The current practice is highly empirical, since it has been difficult to predict the performance of the designed part analytically before it is actually made and tested. It requires the ad hoc use of expertise accumulated over the years and/or expensive time-consuming iterations involving prototype toolings. The short coming of empirical approaches to design and manufacture of injection molds is that the outcome is uncertain since the success of design can be confirmed only through time-consuming prototype testings (Fig. 1 (a)). Furthermore, expertise can be acquired only through prolonged training and accumulation of experience.

The thermo-mechanical history of the molded part and the resulting microstructure must be predicted to evaluate the design analytically prior to actual prototype tooling and testing (Fig. 1(b)). Then the goal of rational design can be accomplished. In order to achieve this goal, a user-transparent, real time flow simulation program and mechanical performance prediction models need to be developed based on most convincing and efficient theoretical models.

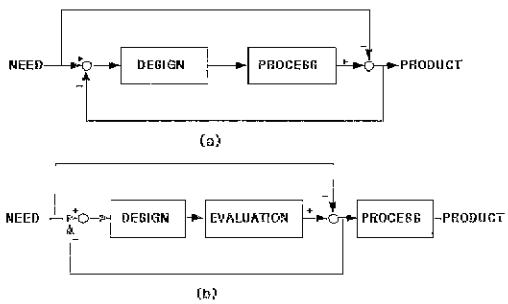

Fig 1 Block diagrams of synthesis
(a) Conventional synthesis
(b) Computer-based rational synthesis

2. Knowledge-based CAE

Since the mid of 1980's, CAE technologies for injection molding have made a big stride by the development of a few commercially applicable mold filling and cooling simulation programs[5]. The diffusion of the injection molding CAE software is further promoted by the powerful computer graphics technology. The control volume method developed by the Cornell Injection Molding Program is the key development among them to transplant the computer graphics technology onto the flow simulation technology[6].The filling pattern of polymer melt, the distribution of the melt temperature, velocity, pressure and volumetric shrinkage can be visualized from the process simulation results However, the result of the analysis cannot be quantitatively used for the mold design evaluation. The mechanical performance of the part, the strength of weldline defects, the occurrence of warpage and dimensional accuracy of the part can only be predicted with human experts' interpretation. Furthermore, the problem in an analytical simulation of the molding process has been the inevitable inclusion of simplifying assumptions in applying theoretical equations expediently to the actual molding process. This makes the accuracy of the analysis for the complex geometry of a mold degraded, notwithstanding the immense computational effort required, leading to a need to build physical prototypes. The task of predicting the mechanical properties of an injection molded part a priori is further complicated due to the coupling between the flow of polymer melts and simultaneous freezing of the plastic during mold filling. Therefore, the use of CAE softwares in injection molding has been limited to a pre-visualization of the melt flow and a few simple qualitative assessments of the post-molding phenomena.

In order to alleviate these kind of difficulties, design evaluation using both the heuristic knowledge and the analytic CAE software has been introduced in this paper. A knowledge-based expert system is one that handles real-world, complex problems which require an expert's interpretation. Therefore, expert mold designers' knowledge can be encoded into production rules of an expert system which can then be used by experts as well as by non-experts in evaluating mold design. A hybrid structure of knowledge-base is constructed to combine the merits of heuristic and analytic knowledge for injection molding.

Hart[7] proposed the multi-level knowledge-base structure to enhance the performance and to eliminate the limits of expert systems. The multi-level structure incorporates heuristic reasonings of surface-level models combined with analytic deep-level models. The surface model is the production rule type system, whereas the

deep model is a purely mathematical description of the physical system. The integration of the analysis programs and the rule-based expert system is the key characteristic of the multi-level knowledge-based system which enables a wide variety of non-expert users to use the sophisticated analysis programs effectively together with formalized heuristic rules.

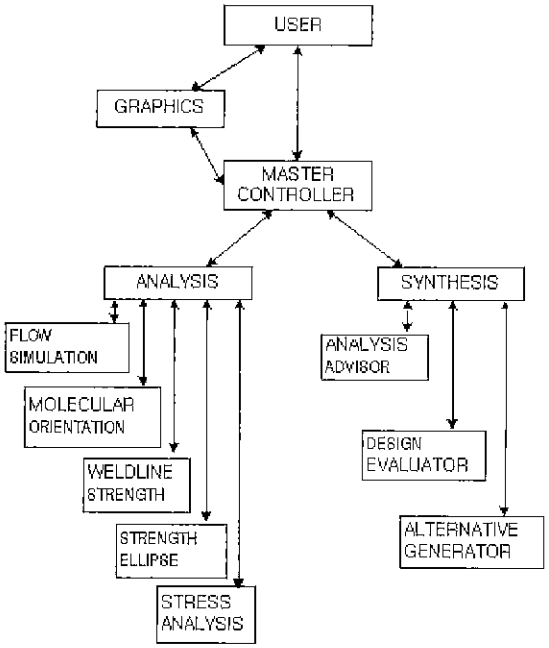

Fig. 2 Functional structure of the knowledge-based synthesis system for injection molding

An expert design evaluation system for injection molding is developed in this study, which has the following multi-level knowledge structure: flow simulation programs for rheological behavior of molten polymers and microstructure analysis programs for solidified polymers, both of which are developed as part of this research, form the deep reasoning model, while a classification model combined with the production system[8] forms the surface reasoning model of the system. Human experts' knowledge in the use of CAE programs and the interpretation of the result is formalized into production rules of the advisory system which also contains the heuristic rules of initial synthesis, evaluation and alternative generation (Fig.2). The knowl edge-based system can diagnose designs based on both the heuristic rules developed from the expert designers' experience and the analytical results of the process simulation. It can also generate optimal alternative designs if the design is not acceptable. The multi-level reasoning structure of the knowledge-based system frees the designer from acquiring detailed knowledge of hydrodynamics, rheology, polymer science and numeri cal analysis which are necessary to run the analysis programs and to interpret the results of them, and provides human experts' knowledge which requires long time to acquire by non-experts.

3. Process Simulation

Injection molded parts have thin, quasi-three dimensional shapes, which can be unfolded to appropriate two dimensional layflats. A two dimensional flow simulation program was developed by Cornell Injection Molding Program for the non-isothermal filling of a thin cavity with variable thickness using generalized Hele-Shaw flow model[9]. It is assumed that inertial effects, streamwise heat conduction and gapwise heat convection are negligible. The fluid is taken to be inelastic, but non-Newtonian under nonisothermal conditions with the shear viscosity assumed to have a power-law shear rate dependence and an Arrhenius-type temperature dependence. The numerical computation is based on a finite element/finite difference scheme in which the planar coordinates are described in terms of finite elements and the gapwise and time derivatives are described in terms of finite difference.

Governing Equations

The Hele-Shaw flow model in a thin cavity has been generalized for an inelastic non-Newtonian fluid under non-isothermal conditions. In the model, the equations of continuity and momentum can be respectively reduced to

$$\nabla \cdot (S \nabla P) = 0 \tag{1}$$

$$u = -\frac{1}{b}\frac{\partial P}{\partial x} S \cdot \quad v = -\frac{1}{b}\frac{\partial P}{\partial y} S \tag{2}$$

where 'b' denotes the half-gap thickness at a location(x,y) and

$$S = \int_0^b \frac{z^2}{\eta} dz \tag{3}$$

Also, the energy equation becomes

$$\rho C_p\left(\frac{\partial T}{\partial t}+u\frac{\partial T}{\partial x}+v\frac{\partial T}{\partial y}\right)=k\frac{\partial^2 T}{\partial z^2}+\eta\dot{\gamma}^2 \tag{4}$$

where

$$\eta=m(T)\dot{\gamma}^{n-1}=A\exp\left(\frac{T_a}{T}\right)\dot{\gamma}^{n-1} \tag{5}$$

$$\dot{\gamma}=\left[\left(\frac{\partial u}{\partial z}\right)^2+\left(\frac{\partial v}{\partial z}\right)^2\right]^{1/2} \tag{6}$$

Finite Element Formulation

Using the divergence theorem, the Galerkin weighted residual equation corresponding to Eq.1 is written as

$$\int_\Omega \Psi_i\nabla\cdot(S\nabla P)d\Omega$$
$$=-\int_\Omega\nabla\Psi_i\cdot(S\nabla P)d\Omega+\int_C[\Psi_i S\frac{\partial P}{\partial n}]dS=0 \tag{7}$$

Interpolating the pressure P, we obtain the following algebraic equation associated with each element in the flow field

$$A_{ij}P_j=R_i \tag{8}$$

The nonlinear equation (Eq. 8) can be rewritten in the following form

$$A_{ij}\delta P_j=R_i-A_{ij}P_j^I \tag{9}$$

$$P_j^{I+1}=P_j^I+\delta P_j \tag{10}$$

where

$$A_{ij}=\int_\Omega S\Psi_{j,x}\Psi_{i,x}d\Omega+\int_\Omega S\Psi_{j,y}\Psi_{i,y}d\Omega \tag{11}$$

$$R_i=\int_C\Psi_i S\frac{\partial P}{\partial n}ds \tag{12}$$

Here, I denotes the number of iteration.

Moving Boundary Problem

In solving a moving boundary transient flow problem, the advancement of the melt front is very important. Once the pressure fields have been determined by Eq. 9 without the cavity boundary information, gapwise-averaged velocity components u and v can be evaluated using Eq. 2. The temperature fields can be found by solving the energy equation (Eq. 4) by finite difference method[9].

In order to complete the filling simulation as a part of the interactive design system, the generation of a new melt front and associated input data preparation at each time step should be done automatically without the user's judgement. In this respect, an automatic mesh generation program for the moving boundary problem is developed as follows.

Consider the current melt boundary $\overline{AB}$ in Fig. 3(a). The predicted melt boundary for the next time step is $\overline{A'B'}$ based on the calculated velocities at the current boundary nodes. However, the advanced boundary falls partly outside of the cavity boundary, which is not physically possible. This is because the forward boundary information is not included in the current calculation of nodal velocities. Therefore, an effort is made to include the forward boundary information in the current calculation. For this purpose, the boundary-pressure-reflection method is derived as follows.

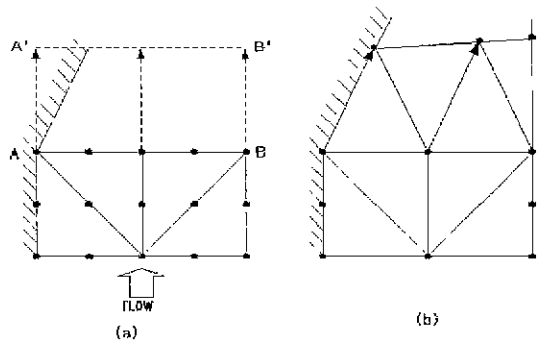

Fig. 3 Automatic melt front advancement
(a) Boundary impingement at the predicted melt front
(b) Regenerated melt front by the pressure reflection scheme

When the melt front impinges partly to the physical boundary, the pressure at nodes near boundary should be redistributed to allow the melt to flow within the cavity. In other words, it is assumed that there exists a virtual pressure at the physical boundary which partly reflects

the current pressure distribution at the nodes near the boundary wall. The magnitude of reflection is dependent on the degree of impingement which represents the magnitude of penetration of the predicted melt front into the solid boundary based on the no-penetration condition The predicted displacement vector, $\overline{R}$, of node 1 in Fig. 4 requires a compensating vector, $\Delta\overline{R}$, to remain on the solid boundary. The degree of impingement is predicted and then reflected to the current pressure distribution near the boundary. The reverse contribution of $\Delta\overline{R}$ to each element is decomposed to ΔU_1 and ΔU_2 by the subtended angle, α and β, and the pressure reflection to each nodal point can be estimated. Then the correct melt front is regenerated, based on the new pressure distribution. Thus the basic idea of the boundary-pressure-reflection scheme is to predict the physically acceptable melt front for the next time step.

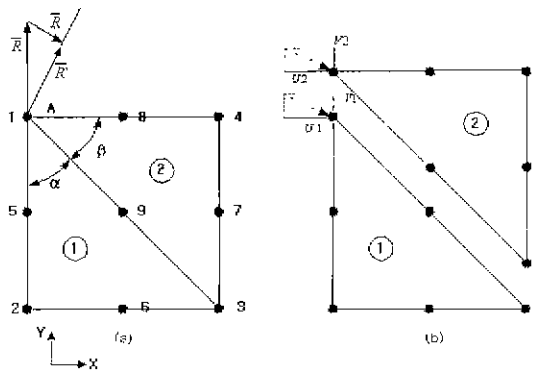

Fig.4 Pressure reflection for two elements containing the boundary node
(a) Degree of impingement
(b) Reflection to each element

After calculating pressure reflections, nodal velocities are recalculated and a correct advanced melt front is predicted based on the recalculated velocities as shown in Fig. 3(b). It is noted that the effect of pressure reflection propagates to only the neighboring nodal points when the nodes of the boundary element are included in the adjacent elements' quadratic shape functions. The idea of boundary pressure reflection has been expanded by Lee, Shin and Kim to cover general impingement cases as follows [10].

Iterative Boundary Pressure Reflection (IBPR) Method

Consider the vector R_i in Eq 12, after the melt front advancement by the use of a predictor-corrector procedure. It is noted that if C_1 designates the portion on which the cavity boundary is satisfied, then the integral along C_1 is zero. On the other hand, if C_2 denotes the portion on which cavity boundary is not satisfied, the contour integral along C_2 cannot vanish. Therefore,

$$R_i = \int_C \Psi_i S(\partial P/\partial n) ds$$

can be regarded as the required boundary pressure reflection vector to satisfy the cavity boundary.

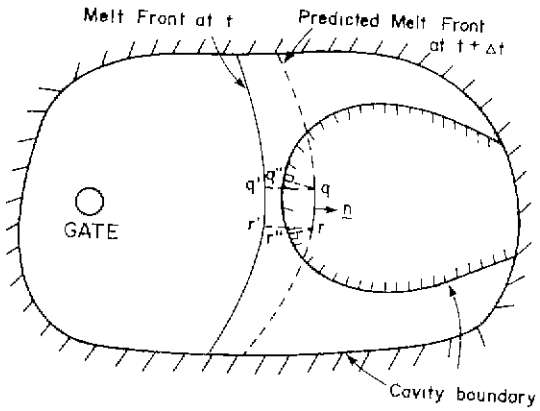

Fig. 5 Impinged shape

The location of the predicted melt front at time t + Δt by the predictor-corrector procedure with no boundary information is shown in Fig. 5. For the sake of convenience, let's consider nodes q and r only. Here nodes q and r were advanced from nodes q' and r' respectively, penetrating into the cavity boundary. Then the required reflected velocity vectors respectively are

$$\overline{v_q} = \frac{\overline{qq''}}{\Delta t} = \bar{u}_q \underline{i} + \bar{v}_q \underline{j} \tag{13}$$

$$\overline{v_r} = \frac{\overline{rr''}}{\Delta t} = \bar{u}_r \underline{i} + \bar{v}_r \underline{j} \tag{14}$$

Along the line $\overline{qr}$.

$S(\partial P/\partial n)$

can be written as

$$S\frac{\partial P}{\partial n}=[S\frac{\partial P}{\partial n}]_q h_q+[S\frac{\partial P}{\partial n}]_r h_r \tag{15}$$

where h_q and h_r are the interpolation functions. Then the nodal boundary pressure reflections at nodes q and r can be estimated as

$$R_q=\int_{S_q}^{S_r}\Psi_q S\frac{\partial P}{\partial n}ds \tag{16}$$

$$R_r=\int_{S_q}^{S_r}\Psi_r S\frac{\partial P}{\partial n}ds \tag{17}$$

Simlarly, on all the impinged nodes, nodal boundary pressure reflections can be estimated using reflected velocity vectors only. After the calculation of nodal boundary pressure reflections, Eq. 9 is solved again. Then new velocities are obtained by the calculated pressure, and a modified melt front is located based on the newly calculated velocities . The modified melt front, however, does not exactly satisfy the cavity boundary by this because the previous pressures are just redistributed by the nodal boundary pressure reflections. Therefore, the scheme also allows iterative calculation to exactly satisfy the cavity boundary.

In updating the front location at each iteration, only pure reflection effect should be considered without time progression. Hence, velocities are calculated at first with zero deflection for the impinged nodes, and then velocities are calculated again with the estimated nodal boundary pressure reflections for the same impinged nodes. Eventually the velocity differences between zero reflection and estimated nodal boundary pressure reflection are used to update the front location at each iteration. Here zero reflection means that the imposed nodal reflection is zero, i.e., R_r=0.

Multiple- Node Impingement

A semi-infinite rectangular cavity with a point gate was chosen as the second test. Fig. 6(a) shows the position of front of the flow field at time t. For a relatively large time increment Δt, the advanced three nodes of the melt front impinge on the cavity boundary at the same time as shown in Fig. 6(b). In this complicated case, the IBPR method is also shown to be very effective as can be seen in Fig. 6(c) and (d). Particularly, it is noted that the effect of reflection has propagated reasonably to the elements far from the impinged nodes.

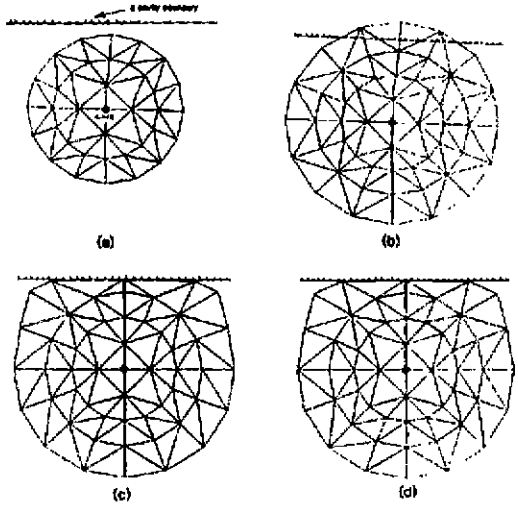

Fig. 6 Iterative reflection scheme
(a) Melt front at t
(b) Predicted melt front at t+Δt
(c) Modified melt front in iteration 3
(d) Converged melt front in iteration 4

The boundary-pressure-reflection scheme provides a theoretical basis for the accurate prediction of a new melt front at each time step. It does not require user's judgements during the regeneration of the melt front. The prediction is based on the correct nodal velocities in which calculation the forward boundary information is included. An automatic mesh generation program is uniquely developed with the idea of the boundary-pressure-reflection scheme which enables the filling simulation to be completed in real time (Fig 7(a),(b)).

The moldability of the design can be readily predicted from the flow simulation by observing a necessary injection pressure during the filling simulation. When the necessary injection pressure does not exceed the limit of the machine's capacity, the design and associated toolings are thought to be adequate to produce the designed part. When the designed part is predicted to be moldable, it is then necessary to predict the mechanical behavior of the molded part. It is done by establishing a thermomechanical data base during the cavity filling simulation. It contains a set of information which is necessary to predict the resulting three dimensional distribution of the microstructural

anisotropies and the mechanical performance of a molded part.

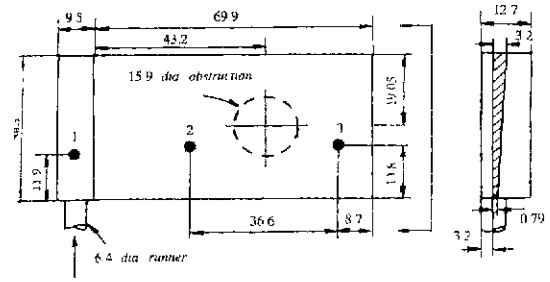

(a)

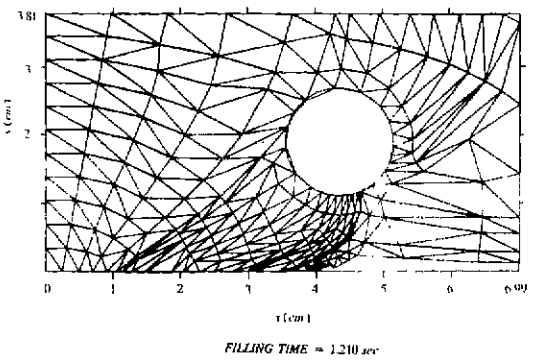

(b)

Fig. 7 (a) Plane view and side view for the cavity including of three pressure transducers : indicated dimensions are in units of mm
(b) Mesh configuration during the filling-simulation (Filling time =1.210 sec)

4. Mechanical Performance Prediction

The mechanical properties of injection molded parts are affected by the microstructural anisotropies within the part since the visco-elastic nature of polymeric materials results in the development of shear and normal stresses. Also the large elastic deformation developed during the filling stage undergoes subsequent relaxation during the packing, cooling, and solidification stage. The resulting microstructures show mixed states of under-relaxed, stretched and crystallized molecular configurations due to the coupling of flow and cooling of polymer melts. This coupling further weakens the molded part via the formation of a weldline structure when melt fronts merge together inside the mold. These two factors, the molecular orientation and the weldline structure, can adversely affect the mechanical behavior of the molded part unless the part and the mold are properly designed.

The molecular orientation, which is often inherent to polymer processing techniques, has received considerable theoretical and experimental investigations [11,12]. The effect of molecular orientation on the mechanical properties of a molded part is most likely to be deteriorative, revealing themselves in the form of crazing under stress, or the loss of strength when subjected to transverse stresses(Fig.8). This is due to the very weak intermolecular bond between molecular chains in comparison to the strong covalent bond along the backbone chain. The more the molecular chains are stretched, the higher energy barrier the longitudinal deformation has and the lower energy barrier the transverse deformation has. Therefore, the anisotropic mechanical strength can be predicted by calculating the degree and direction of the frezen-in molecular orientation from the thermomechanical data base generated during the flow simulation.

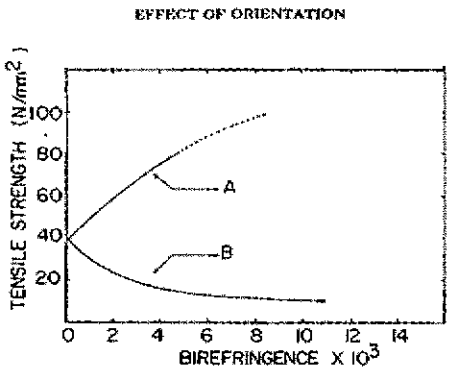

Fig. 8 The effect of molecular orientation on the tensile strengths of polystyrene
A: Longitudinal strength
B: Transverse strength

Dietz and White[13] developed a prediction model for the molecular orientation based on a set of assumptions. They assumed that the state of the polymer melt consists of an isothermal core region and solidified layers in the wall region. Based on their model, an isothermal power-

law flow model is applied in the core region and the birefringence at the melt-solid boundary is calculated which is to be the frozen-in orientation due to the instantaneous solidification of the melt at the boundary. The growth of the frozen-layer thickness is successively calculated until the whole cavity is filled. After the cessation of flow, non-isothermal stress relaxation is considered by means of a simple Maxwllian-type model in which the relaxation time is not a function of shear rate, but only a function of temperature. The corresponding birefringence, which is the measure of orientation for amorphous polymers, is then calculated by multiplying the stress optcal coefficient to the calculated principal stress difference on the basis of the stress optical law[13] as:

$$\Delta n = C\sqrt{4\tau_{12}^2 + (\tau_{11} \cdot \tau_{22})^2} \tag{18}$$

where C is the stress optical coefficient, τ_{12}, and τ_{11}, τ_{22} are the shear stress and normal stresses respectively. For polystyrene, the stress optical coefficient, $C=4.9*10^{10}$ cm^2/dyne as measured by Wales [12].

By comparing the experimental measurements of birefringence with the theoretical models, a similitude in the pattern of gapwise birefringence at each location of the molded part are observed. It can be characterized by four local min/max points in the magnitude of cross sectional molecular orientation. Their locations are the surface, the immediate skin layer, the melt/solid boundary at the end of filling, and the center which has the most time to relax its orientation.

(1) A local maximum of birefringence at the surface which is mainly determined by the elongational flow at the melt front. As soon as the advancing melt front which spills from the center toward the wall touches the cold mold wall, the elongational stress is frozen-in to the surface without relaxation. The principal stress difference can be calculated from the fountain flow model as[13].

$$\Delta\sigma_0 = \Psi_e \dot{\varepsilon} \tag{19}$$

where ψ_e is the extensional viscosity of the melt and $\dot{\varepsilon}$ is the rate of elongation.

(2) A local maximum of birefringence at the location which coincides with the thickness of the solidifying layer at the instant of complete filling. This can be calculated by applying the simple shear flow model along the streakline with known temperature profiles and the melt front arriving time which have been predicted from the filling simulation. At the instant of complete filling, the thickness of the solidified layer is the half-gap thickness. Then the shear stress at the melt-solid boundary is

$$\tau_{12} = m_c \dot{\gamma}^n \tag{20}$$

$$\dot{\gamma} = \frac{2n+1}{n}\frac{V}{H - H_s} \tag{21}$$

where m_c is the shear viscosity, $\dot{\gamma}$ is the shear rate at the melt-solid interface, and n is the power law index[13].

(3) There is a local minimum point between the surface and the internal maximum point. This is resulted by overlapping of the increasing shear stress on the diminishing elongational stress which was originated from the fountain flow of the advacing melt front. It is observed that the local minimum location is very close to the surface in general. Therefore, a linear interpolation is employed in this study between the surface birefringence and the maximum birefringence at the melt-solid interface.

(4) The magnitude of birefringence inside the melt core region is dependent on the cooling rate which is usually determined by the thickness of the part and the temperature of the mold. Incomplete relaxation of the shear stress remains as the residual stress which can be approximated as a quadratic distribution. It is assumed in this study that the center of the core region is fully relaxed.

Based on this similitude model, the gapwise distribution of molecular orientation can be predicted simply by calculating the maximum birefringence from the shear flow analysis and the surface birefringence from the elongational flow analysis. In order to compare the result of simplified prediction with other experimental and theoretical data[9,12,13], a rectangular cavity, as shown in Fig. 9 is chosen and the simplified procedure is applied to it. Curve (a) in Fig. 9 is the experimentally measured birefringence by Wales[12]. Curve (b) is the predicted birefringence pattern by Dietz and White[13]. Curve (c) is calculated by Isayev, Shen and

Hieber[14]. Curve (d) is the pattern predicted in this paper. The approximation employed in this study is proved to be a reasonable method to predict the gapwise pattern of molecular orientation, while reducing the computation effort enormously.

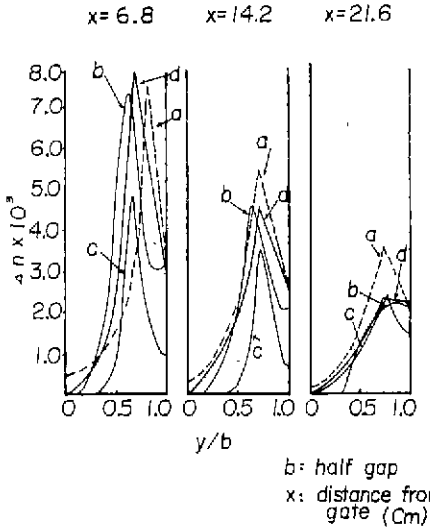

Fig. 9 Gapwise birefringence pattern in rectangular cavity: (a) Experimental measurement results in reference 12 (b) Prediction results in (13) (c) Prediction results in reference 14 (d) Prediction results in this study

Theoretical models of the molding process and the generation of molecular orientation and its effect on mechanical properties are well established[11,12,15]. However, there are some important mechanical anisotropies which have not yet been predicted quantitatively, although their phenomenological aspects are well understood. One of these anisotropies is caused by weldlines. Weldline is one of the most serious defects which must be considered at the design stage[17]. The presence of a weldline generally reduces the mechanical strength of injection molded parts. Therefore, a theoretical model for the strength of weldline was presented by the authors[17], which provided a comprehensive physical insight of the bonding process at the weldline interface. The model is based on the self-diffusion of entangled molecular chains across the polymer-polymer interface and the frozen-in elongational molecular orientation which remains parallel to the interface. The degree of bonding due to the molecular interdiffusion across the weldline interface is derived as;

$$\frac{\sigma_w}{\sigma_b} = 1 - \frac{A}{A_0}$$
$$= 1 - \exp\{-\frac{CD}{kT}(2\dot{\gamma} - \frac{0.98}{\sqrt{2}}kT\delta n_0 \delta x)t\} \quad (22)$$

Where σ_w, σ_b are the strength of weldline and the bulk respectively. T is the interface temperature, t is contact time and others are material constants. Both factors are analyzed separately and then superimposed to predict the strength of weldlines from known processing conditions and geometry Experimental results show good correlation with predictions(Fig 10).

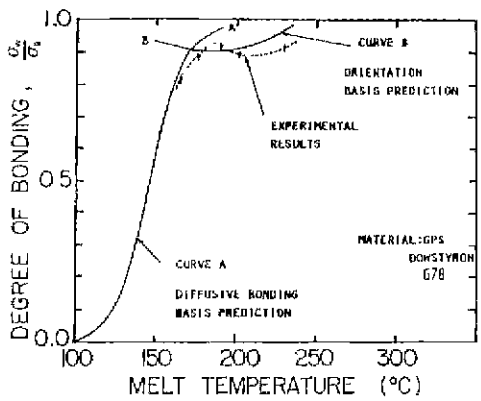

Fig. 10 Theoretical prediction and experimental results of the tensile strength at the weldline of amorphous polystyrene[12].

A spatial distribution of the frozen-in molecular orientation inside a molded part and the strength of weldlines can be predicted from known processing conditions based on efficient but convincing theretical models developed in this research. In order to be used for design evaluation, a condensed form of mechanical performance index which represents the anisotropic properties of a molded part is required.

Consider a sufficiently small planar element as an orthotropic laminae It is assumed that the laminae represents the local distribution of the microstructure at a certain location of a thin injection molded part. It is also assumed that the major orientation occurs along the flow direction[17] and the averaged molecular orientation along

the thickness represents the magnitude of the anisotropic microstructure of the laminae as shown in Fig.11. For the idealized orthotropic laminae under a plane stress condition, the Tsai-Hill failure criterion[18] is applied to determine the strength locus as follows;

$$(\frac{\sigma_L}{\sigma_L^*})^2 - (\frac{\sigma_T \sigma_L}{\sigma_L^{*2}}) + (\frac{\sigma_T}{\sigma_T^*})^2 + (\frac{\tau}{\tau^*})^2 = 1 \qquad (23)$$

where σ_L^* is the tensile strength of the material along the orientation, σ_L is the longitudinal tensile stress. Likewise, σ_T^* is the transverse tensile strength, σ_T is the transverse tensile stress, τ^* is the shear strength of the laminae and τ is the shear stress.

The shear strength, τ^* , can be obtained via off-axis tests[18]. As an effort to determine the relation between the shear strength and the molecular orientation, the experimental results of tensile test by Hoare and Hull[19] are used instead of the off-axis test. However, due to the mixed mode fracture in the range of angle, 20 deg.<θ<70 deg., the shear strength cannot be obtained from the experimental results as the orientation increases. Therefore, the explicit form of the Tsai-Hill criterion cannot be used in this application. Furthermore, it has been proved experimentally that the longitudinal tensile fracture occurs in the range of angle, 0 deg.< θ <20 deg , and the transverse tensile fracture occurs in the range of angle, 70 deg.< θ <90 deg. regardless of the shear strength.

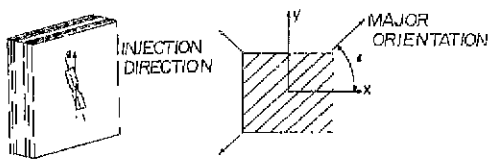

Fig. 11 Injection molded part as a composite laminae

A simplified form of strength ellipse is proposed in order to represent effectively the spatial distributions of anisotropic properties within a molded part and to compact the microstructural database of them.

$$(\frac{\sigma_L}{\sigma_L^*})^2 + (\frac{\sigma_T}{\sigma_T^*})^2 = 1 \qquad (24)$$

The major axis of the ellipse by Eq. 24 represents the major direction of the molecular orientation. The intercept on the major axis represents the longitudinal tensile strength and the intercept on the minor axis represents the transverse strength as shown in Fig. 12. In the graphical form of a strength ellipse, the magnitude and the direction of the molecular orientation within a molded part and its effect on the mechanical strength of the part are represented comprehensively.

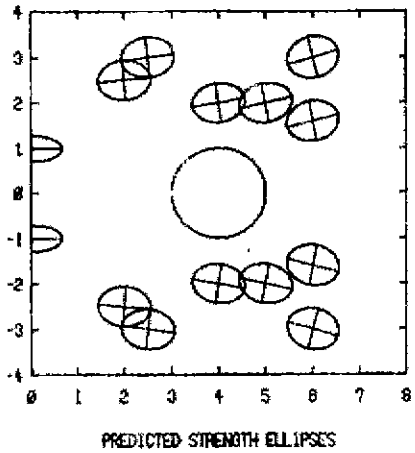

Fig. 12 Predicted strength ellipses at different locations. Major axis represents the stretched direction and major and minor axes represent longitudinal and transverse tensile strength

5. Knowledge Formalization

EXSYS is a general purpose expert system which provides a basic framework for designing a specific expert system developed by EXSYS incorporation. It is one of the simpler systems and is specialized for classification type applications. It is written in C, which makes communication between the expert system and the external analysis programs relatively straightforward. Heuristic rules of design for injection molding are formalized and implemented as production rules according to the EXSYS' language structure. They are based not only on human experts' experience but also on the result from analysis programs.

Design Evaluation

Moldability of a designed part can be readily determined from the result of the flow simulation. When the necessary injection power during the flow simulation

exceeds the limit of the employed injection molding machine, it can be concluded that the flow path is blocked by the pre-solidification of polymer melt. This results in a short shot of the part and the designed part is not moldable. Therefore, the first criterion for design evaluation is set as follows:

- **Moldability**

  When the required injection power exceeds the limit of the machine's capacity, short shot occurs and the designed part is not moldable.

The global mechanical behavior of the designed part can be determined by comparing the result of analysis for stress distribution due to an externally applied load and its effect on the mechanical anisotropies predicted for the entire geometry. However, this requires an immense amount of computation time and data storage. This problem can be alleviated by using a heuristic method to avoid the brute force analysis in evaluating mechanical acceptability of the design.

It has been observed by experts that mechanical failures start where stresses are concentrated at the weakest directions of mechanical anisotropies. For arbitrary loading situations, stress concentrations occur at holes, corners, edges and thin sections. Therefore the distribution of microstructural anisotropies at these regions are critical in determining the critical mechanical behavior of the part. Form the above observation, the second criterion is deduced for evaluation the mechanical performance of molded parts as follows:

- **Mechanical Acceptability**

  An adverse combination of microstructure and geometry is the principal cause of the mechanical failure of an injection molded part.

A local prediction scheme which checks the microstructure only at critical locations of the designed part is developed based on this rule. The microstructures and accompanying an isotropic properties are predicted at regions pre-selected based on possible occurrence of stress concentration. Then the acceptability of the design is judged using production rules.

Design Alternative Generation

Human experts have developed simple and intuitive design rules based on years of trial-and error testing experience. As an effort to formalize the empirically acquired remedies as production rules, the causal relationship between the design variables, thermomechanical properties, and the resulting microstructural anisotropies are studied. Fig. 13 shows the schematic causal relationships based on the experimental and theoretical work of many researchers [15,18]. Although the individual relationship cannot be identified explicitly due to the strong coupling among them, a general causality is observed as follows:

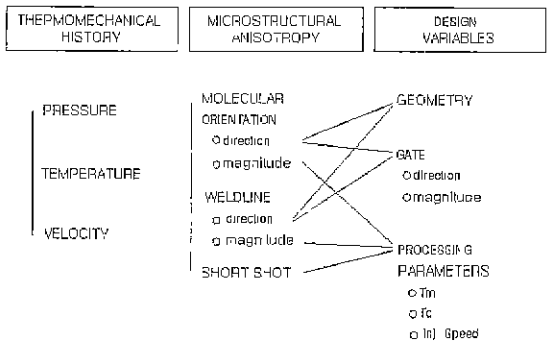

Fig. 13 Causal relations between major design variables and microstructural anisotropies.
Solid lines mean strong causality.

- **General Causality**

  – The direction of the anisotropy is mainly dependent on the geometrical variables, such as, the primary part shape, the secondary part shape, type and location of the gate.

  – The magnitude of the anisotropy and the moldability is mainly dependent on thermal and temporal variables of the process, such as, melt and mold temperature, and injection rate.

Although the general causality is not a theoretically induced fact, it can be effectively used in generating design alternatives together with the evaluation criteria established above. By integrating the heuristic observations and the analytical predictions, decision rules for design diagnosis and redesign is formulated in Fig. 14.

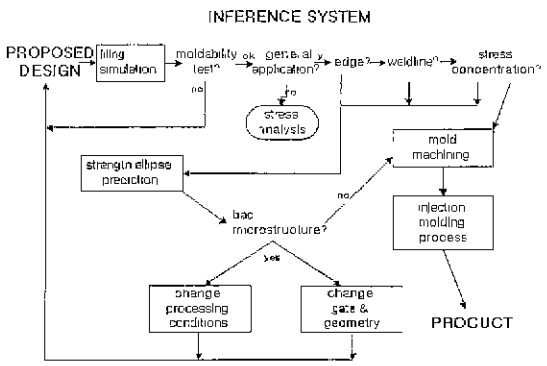

Fig. 14 Decision rules for design diagnosis and redesign. Both the analytical results and empirical findings are integrated into this inference engine.

6. Evaluation System

A prototype knowledge-based synthesis system (Fig. 15)is built based on performance prediction programs and the production rules which are formalized in previous section (Fig. 14).

The use interacts with the synthesis system via the master controller. The master controller receives initial design information from the user and triggers the expert system to request an advice for the next action. Depending upon the decision from the expert system, the controller either executes the analysis programs or returns the decision of the expert system to the designer for additional questioning or conclusions.

The expert system has three major functional blocks: data retrieval and synthesis control, design evaluation, and redesign advice. Based on the information supplied by the master controller, it interprets the data and decides the necessary actions for the controller If the supplied information is not sufficient to evaluate the design or to confirm the conclusion, the expert system requests the controller to take relevant action to obtain more data either from the user or from the analysis programs. After retrieving sufficient information to evaluate the design. It diagnoses the design and generates proper alternatives.

The analysis system has five functional blocks as shown in Fig. 2. Flow simulation is the core of the analysis system because it generates a necessary thermo-mechanical data base for further analyses. Therefore, it is executed whenever a design change is made. Moldability is readily predicted from the result of the

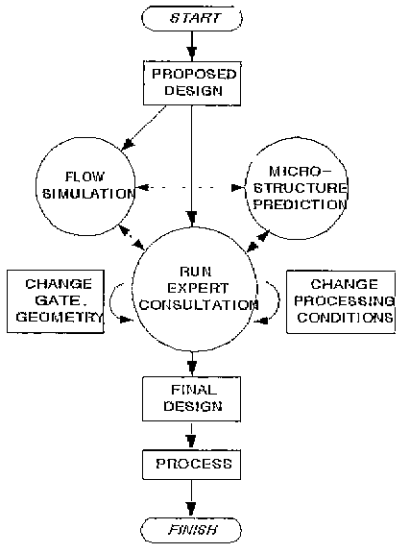

Fig.15 The prototype expert synthesis system for injection molding

flow simulation Mechanical performance prediction programs are executed only when the expert system requests the running of the specific program among them.

For a more realistic case study, an L-shaped cavity with an insert at the center and varying thickness is designed as shown in Fig. 7(a) The part is then unfolded as a lay-flat and the two dimensional cavity filling simulation is carried out with the assumption the melt is injected through a fan gate. Processing parameters and constants are as follows:

Melt Temperature: 493K
Mold Wall Temperature: 303K
Injection Rate: 10.0 cm^3/sec(whole cavity)
Material: polystyrene

For a given design task, the flow simulation program is first executed to build a thermomechanical data base. Advanced melt fronts are generated automatically at each time step as shown in Fig. 7(b).

Then the expert consultation program is initiated. Based on the decision from the expert system, a part or the whole of the microstructure analysis programs is executed. The expert system's request with relevant data for a specific analysis program is transmitted to the microstructure analysis system via communication programs between the expert system and the microstructure analysis program. Predicted strength

ellipse shows the magnitude and the direction of the resulting mechanical anisotropy at locations where the expert system specifies (Fig. 12). The result of the analysis, then, automatically returns to the expert system to diagnose the design. If the design is not acceptable, the user generates an alternative solution based on expert system's advice. The expert system diagnoses finally that the weldline along the edge should be avoided by changing the gate position in this case study(Fig. 7(a).(b)). The design cycle is repeated until the acceptable design is made.

7. Conclusion

A knowledge-based synthesis system is built to embody the goal of a rational design by integrating two domains of knowledge of injection molding. Heuristic knowledge of design is formalized as production rules and combined with analytical knowledge from the process simulation. Theoretical models for predicting the moldability of the design and the mechanical performance of the molded part have been formulated.

The overall structure of the expert system, as designed, is based on EXSYS, which is an expert system designing tool, and linked together with analysis programs to have a multi-level reasoning structure. The synthesis system can diagnose the design and direct the designer to reach the optimum design based on the accumulated human experts' knowledge and the most convincing theoretical models of the process which are hard to acquire by non-expert designers.

The origins of molecular orientation and weldline, and their effect on the mechanical strength are well characterized. By employing a reasonable approximation with convincing mathematical models of one dimensional shear and two dimensional elongational flow, the spatial variations of molecular orientation and accompanying mechanical strength are successfully predicted. The direction of major orientation and the magnitude of longitudinal and transverse tensile strength are effectively represented by a simple form of strength ellipse. The shape of the strength ellipse can be used as an intuitive design index which represents the state of microstructural anisotropies within a molded part.

The current knowledge base contains decision rules and mathematical models only with respect to moldability and mechanical acceptability of the design. More knowledge about the injection molding process must supplement the current knowledge base in order to evaluate and modify designs in every aspect of injection molding, such as, sinkmarks, jetting, warpage, and mold design, among others

References

1. Suh, N.P., "Manufacturing and Productivity," Key note paper at the Sagamore Conference, 1984.
2. Rinderle, J.R., "Measures of Functional Coupling in Design," Ph D Thesis, MIT, 1982.
3. Suh, N.P., Bell, A.C. and Gossard, D.C., "On An Axiomatic Approach to Manufacturing Systems," Journal of Engineering for Industry, Trans. ASME Vol.100, No.2, May, 1978.
4. Winston, P.H., "Artificial Intelligence," Addison Wesley, 1984.
5. Manzione, L. T., "Applications of Computer Aided Engineering in Injection Molding," Hanser Publishers, 1987.
6. Wang, V.W., et al, "Dynamic Simulation and Graphics for the Injection Molding of Three Dimensional Parts," Journal of Polymer Engineering, pp. 21-45, 1986.
7. Hart, P., "Directions for Artificial Intelligence in the Eighties," *SIGNART News letter 79:11-16, 1982.*
8. Weiss, S. M., Kern, K. B., et al., "A Guide to the Expert Consultation System," Technical Report CBM-TR-94 Rutgers University, December, 1984.
9. Hieber, C. A. and Shen, S. F., "A Finite-Element, Finite-Difference Simulation of the Injection-Molding Filling Process," Journal of Non-Newtonian Fluid Mechanics 7, pp. 1-32, 1980.
10. Kim, S. G., Huh, Y. J., Shin, H. C., and Lee, H. S., "Development of an Expert Design System for Injection Molding," Korea Institute of Science and Technology Research Report, 2N328-3157-7, 1988.
11. Curtis, J. W., "The Effect of Pre-orientation on the Fracture Properties of Glassy Polymers," Journal. of Physics D: Appl, Phys, 3:Vol.3, 1970.
12. Wales, L. L. S., "The Application of Flow Birefringence to Rheological Studies to Polymer Melts," Delft Univ. Press, 1976.
13. White, J. L. and Dietz, W., "Some Relationships

between Injection Molding Conditions and the Characteristics of Vitrified Molded Parts." Polymer Engineering and Science Vol. 19, No. 15, 1979.

14. Wang, k. k., et al, "Computer Aided Injection Molding System", Technical Report 2-10, Cornell Injection Molding program.
15. Kim, S. G., "Knowledge-based Synthesis System for Injection Molding," Ph D thesis MIT, 1985.
16. Kim, S. G. and Suh, N. P., "Performance Prediction of Weldline Strength in Amorphous Polymers," SPE 42th ANTEC Technical Papers, New Orleans, May, 1984.
17. Menges, G. and Wubken, G., "Influence of Processing Conditions on Molecular Orientation in Injection Moldings," SPE 31st ANTEC, Montreal, May, 1973.
18. Hull, D., "An Introduction to Composite Materials." Cambridge Univ. Press, 1981.
19. Hoare, and Hull, D., "The Effect of Orientation on the Mechanical Properties of Injection Molded Polystyrene," Polymer Engineering and Science, Vol. 17, No. 3, March, 1977.